Vilnius University
Faculty of Physics

Yahya Khurshid Malik

COMPOSITES WITH NANO INCLUSIONS FOR ELECTROMAGNETIC APPLICATIONS

Master's final thesis
Electronics and Telecommunication engineering

Student	Yahya Khurshid Malik
Approved	2021-05-20
Academic supervisor	dr. Jan Macutkevic
Director/ representative of the Institute / Center	prof. Robertas Grigalaitis

Vilnius 2023

Table of Contents

Abstract
The aim of the research is to study the impact on key electromagnetic properties such as permittivity, permeability, and dielectric loss was studied using a systematic approach. Composites were made using carefully selected nano-sized particles. The presence of nano inclusions improves the electromagnetic properties of the composites significantly, based to the findings. Significantly, increased permittivity and permeability have been observed, resulting in improved wave absorption, shielding effectiveness, and energy harvesting capabilities. These advancements hold promise for a variety of applications, including antenna design, electromagnetic shielding, and energy harvesting techniques that are effective.

1 Introduction

In the field of electromagnetic applications, composites containing Nano inclusions have drawn a lot of interest because of their distinctive characteristics and multifaceted usefulness. These composites, also known as nanocomposites, are made up of a matrix material with nanoscale inclusions, some of which can be carbon-based, others of which can be metallic, ceramic, or other materials. Here are a few instances of Nano inclusion-containing composites utilized in electromagnetic applications:

1. Carbon nanotube (CNT) composites: carbon nanotubes are strong and have high electrical conductivity. CNT composites show improved electrical conductivity, electromagnetic interference (EMI) shielding efficiency, and outstanding microwave absorption properties. They are employed in things like electromagnetic waveguides, radar-absorbing coatings, and EMI shielding materials[1].
2. Graphene composites: a hexagonal lattice of carbon atoms is laid out in a two-dimensional sheet to form graphene. A composite material's electrical conductivity, thermal conductivity, and mechanical characteristics are all improved by the addition of graphene. Graphene composites are used in supercapacitors, antennas, conductive coatings, and EMI shielding [2].
3. Magnetic Nanoparticle Composites: magnetic nanoparticle composites may be made by propagating magnetic nanoparticles in a polymer matrix, such as nickel zinc ferrite ($NiZnFe_2O_4$) or iron oxide (Fe_3O_4). These materials are appropriate for uses including magnetic sensors, electromagnetic wave absorption, and magnetic shielding because they have good magnetic characteristics [3].
4. Metamaterial Composites: fabricated composite structures known as metamaterials have special electromagnetic characteristics that are not present in materials that are naturally occurring. Metamaterial composites can display characteristics like negative refractive index, almost zero permittivity, and good impedance matching by integrating nanoscale inclusions with certain shapes and arrangements. They are used in high-frequency gadgets, cloaking devices, and antennas [4].
5. Ceramic Matrix Composites: for their dielectric qualities, ceramic composites containing nanoscale inclusions like alumina, zirconia, or barium titanate are used. These composites are used in products including capacitors, high-frequency circuit substrates, and microwave

devices because they have high dielectric constant, low dielectric loss, and excellent insulating qualities.

1.1 Allotropes of carbon

Primary carbon allotropes are:

1) Diamond

Carbon atoms are laid out in a hard, clear crystal lattice to form diamond. For their extraordinary hardness, brightness, and usage in jewelry, diamonds are known.

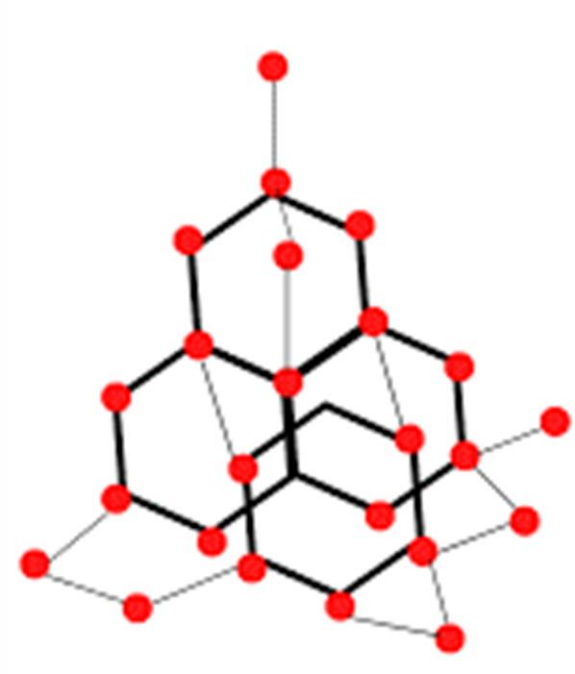

Figure. 1 Structure of diamond.

2) Graphite

Graphite is a soft, dark material made up of layers of hexagonally organized carbon atoms. [6].

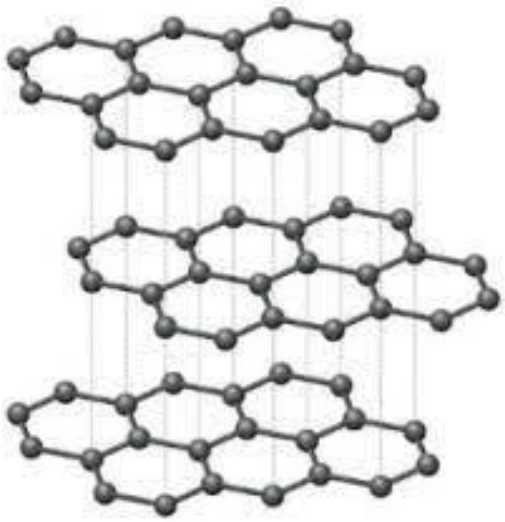

Figure. 2 Structure of graphite.

3) Fullerene

Carbon atoms can be arranged in hollow spheres, ellipses, or tubes to make fullerene molecules. The most well-known fullerene, C60, has a soccer ball-like form.

These carbon allotropes are useful in a variety of sectors and scientific study because of their unique shape and characteristics [7].

The aim of the work is to compare electrical properties of epoxy resin and biobased composites with carbon nanoinclusions and to investigate electrical properties of biobased and iron oxide nanoparticles in wide 20 Hz – 2 THz frequency range.

2. Literature review

2.1 Electrical Percolation

When a substance transforms from not being conductive to being so, the electrical percolation takes place. When the material's conducting elements are sufficiently concentrated or connected, it happens. If the conducting elements are scattered and isolated below a certain point, electrical current cannot flow. As the concentration rises, the various conducting components begin to come together, creating a path for electricity to flow. The electrical percolation refers to the conversion from insulating to conductive [8]. Designing materials with particular electrical properties is of great importance for uses like electronics and energy storage. The primary point at which this transformation takes place is the percolation threshold. Controlling and improving the electrical characteristics of materials, especially composites, requires a thorough understanding of electrical percolation phenomena [9].

When describing how a material's electrical properties change with frequency, there are basically two types of models that are applied:

1) Debye Relaxation Model

This model takes into account the alignment of polar molecules in response to an electric field to explain the frequency dependence of permittivity [10]. It is presupposed that the substance is made up of these polar components capable of aligning with the field. The alignment of these dipoles is described in the model by a single relaxation period τ, called the Debye relaxation time.

$$\varepsilon^* = \varepsilon_{inf} + \frac{\Delta\varepsilon}{1+i\omega\tau} \quad (1)$$

Where $\varepsilon^*=\varepsilon'-i\varepsilon''$ is the complex dielectric permittivity, ε_{inf} is the dielectric permittivity at very high frequencies, $\Delta\varepsilon$ is the dielectric strength.

2) Cole-Cole model

When the material displays more complex behaviour, the Cole-Cole model, a modified version of the Debye model, is applied [11]. It allows for a more accurate description of materials with numerous relaxation processes taking place at once since it considers a range of relaxation

durations rather of just one with symmetric distribution of relaxation times and distributions width α:

$$\varepsilon^* = \varepsilon_{inf} + \frac{\Delta\varepsilon}{1+i\omega\tau^{1-\alpha}} \quad . \tag{2}$$

Both of the models helps in the understanding of how the electrical characteristics of a material, such as conductivity and permittivity, change when the frequency of the applied electric field changes[12]. They are frequently employed in the research of polymers, dielectric materials, and other systems where the frequency of the supplied signal affects the electrical behavior [13].

2.2 Electromagnetic shielding

A method to stop or lessen the impact of electromagnetic waves is electromagnetic shielding. It involves applying substances or structures that can block or restrict these waves [14]. This is helpful because electromagnetic waves have the potential to damage human health or interfere with electronic devices [15]. Utilising materials like metal or unique alloys that can deflect or absorb waves is shielding. It is applied in a number of industries to safeguard delicate machinery, provide communication privacy, and lower health risks.

2.3 Electromagnetic Interference (EMI)

When unwanted electromagnetic signals prevent or disrupt the correct working condition of electronic systems or devices, this is known as EMI. It may arise from radio frequency sources, power lines, electronic devices, lightning, and other unexpected events. In devices that are affected, EMI may result in errors, malfunctions, or decreased performance [16]. Electromagnetic shielding, filtering, grounding, and electromagnetic compatibility (EMC) design are some of the approaches used to reduce EMI. Materials are used in electromagnetic shielding to block or reroute electromagnetic waves. In order to reduce unwanted signals, components are used in filtering. Interference is reduced with appropriate bonding and grounding. Devices are designed with EMC considerations to reduce EMI generation and ability to react [17]. In sectors like telecommunications, electronics, aerospace, automotive, and healthcare, EMI reduction is essential.

2.4 Electromagnetic Radiation

Waves of energy called electromagnetic radiation move through space. It has various frequencies and wavelengths. When it comes into contact with materials, it can be absorbed, transmitted, reflected, or scattered [18]. The speed of light is the constant rate of electromagnetic radiation in a vacuum. As a result of its interactions with matter, it may produce electric currents, heat, or chemical changes. There are many uses for electromagnetic radiation, including communication, lighting, imaging in medicine, and many more [19].

The visible light spectrum, which ranges in colour from red to violet, is the form of electromagnetic radiation that the human eye is able to detect. The wavelengths in this range are roughly between 400 and 700 nanometers. Cones, which are photoreceptor cells located in the eye, are in charge of detecting this light and turning it into electrical impulses for vision. However, other types of electromagnetic radiation like X-rays, gamma rays, ultraviolet and infrared light cannot be seen by the human eye. Because the power density of an electromagnetic wave correlates to the inverse of the square of the distance from the source, doubling the distance from a transmitter will cause the power density of the radiated wave to drop to 1/4 of its previous value [20].

2.5 Radio waves

Broad wavelengths and low frequencies are characteristics of radio waves, a category of electromagnetic radiation. They are a type of non-ionizing radiation that is frequently employed in radar, broadcasting, and wireless communication systems [21]. Radio waves usually operate at frequencies within interval of 3 kilohertz (kHz) and 300 gigahertz (GHz), with wavelengths that vary between a few centimeters to thousands of kilometers.

A variety of devices, such as antennas, transmitters, and oscillating electric charges, are capable of creating radio waves. Until they run into obstructions or are affected by reflection, refraction, or diffraction, they move through the surrounding environment and the air in a straight line [22].

Due to their low frequency and relatively low atmospheric absorption, radio waves have important characteristics that allow them to travel over long distances and around obstacles. They are suitable for long-distance communication because of this characteristic.

Radio broadcasting, television transmission, wireless communication systems (like Wi-Fi and Bluetooth), mobile phones, satellite communication, navigation systems (like GPS), and weather radar are just a few of the uses for radio waves. Within particular frequency bands designated for various uses, every device runs [23]. They are extremely useful for multiple uses in present-day technology because of their long wavelengths, low frequencies, and ability for travelling great distances.

2.6 Electromagnetic compatibility testing

Electromagnetic compatibility testing, or EMC testing, is a procedure that assesses an electronic device's capacity to operate effectively without producing or being impacted by electromagnetic interference. It involves evaluating electromagnetic emissions, sustainability to additional electromagnetic fields, and potential to disturbances like power surges and electrostatic discharges. EMC tests are carried out in specialized labs with standardized processes and calibrated tools [24]. It guarantees that equipment can function dependably and live side by side with other equipment without causing electromagnetic interference. EMC compliance is crucial for quality assurance and market access across a variety of industries.

2.7 EMC tests can be divided into immunity tests and emissions tests.

The main goal of emissions testing is to assess a device's electromagnetic emissions. It measures electromagnetic energy that is conducted and radiated to make sure that it stays within the legal and acceptable bounds. The reason for this is to stop the device from interfering with nearby devices.

On the other hand, immunity testing evaluates how resistant the device is to outside electromagnetic disturbances. In situations where there is electromagnetic interference from sources like radio frequency fields, electrostatic discharges, power surges, and conducted disruptions, it analyses how well the device can operate normally and remain unaffected [25].

3. Experiment

3.1 Measurements in 20 Hz – 3 GHz frequency range

Using an LCR meter HP4284 A, dielectric properties between 20 Hz and 1 MHz were measured. Contacts were painted with silver paint.

In the frequency 1 MHz – 3 GHz, dielectric measurements were performed using a vector network analyzer Agilent 8714ET.

3.2 Microwave reflectivity and transmission measurements

Thin cylindrical rod in rectangular waveguide technique was used for dielectric measurements in the centimeter and millimeter microwave ranges. Using an automatic dielectric spectrometer, the moduli of the microwave reflection and transmission coeficients were measured. The moduli of microwave reflection and transmission coeficients were measured in the frequency range from 20 GHz to 55 GHz using generators as variable frequency sources and changing only the waveguide terminating with a matched load. Range bandwidth is influenced by waveguide wall width and microwave oscilator bandwidth. For measurements of reflection, transmission, and supporting power, a scalar network analyzer is employed. Digital analog converters, used to change the frequency of generators, are located in the interface unit. With the exception of K-61, where this function is linear, the signal level of digital analog converters' generators was measured with a frequency cell and described as a third order polynomial.

The cylinder-shaped sample was positioned in the middle of the broad waveguide wall, perpendicular to the electrical field of the primary TE10 modes. It was done using a unique sample holder. There is a piston slot in this sample holder. There is a notch in the piston for the sample that is used for contacts between the sample and the waveguide. For the calibration of reflections and transmissions, two additional pistons were used. In addition to allowing the chance to confirm a calibration during an experiment, this method allows for the rejection of waveguide channel destruction.

.

The dependence of the reflection and transmission coefficients on a real portion of the dielectric permittivity becomes weaker as dielectric losses rise, which together reduce the method's accuracy.

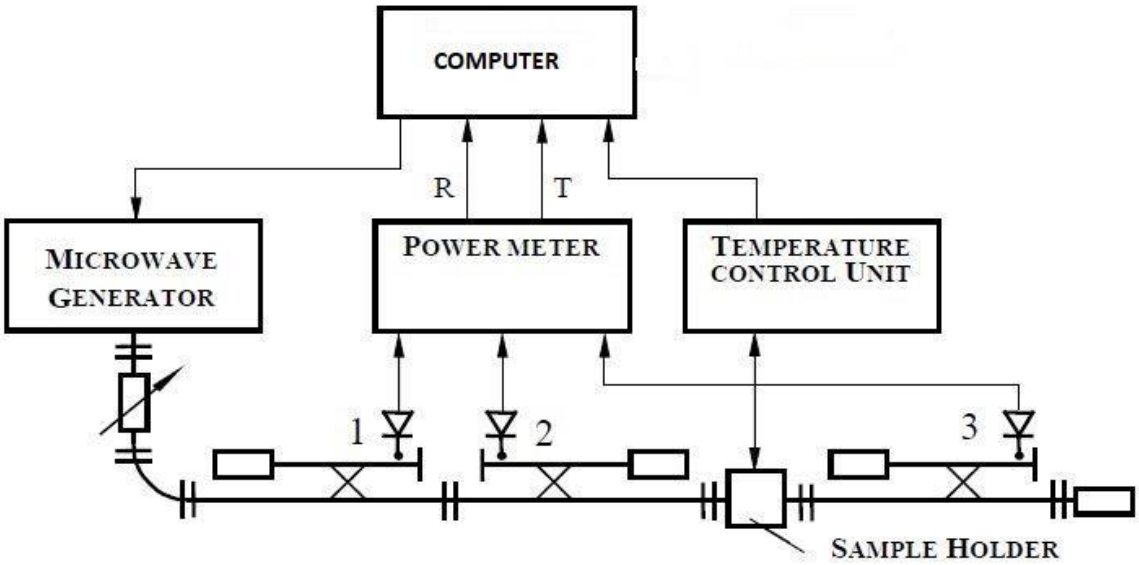

Figure. 3 Dielectric spectrometer setup for reflection and transmission measurements

3.3 Samples

3.3.1 Bio-based electro conductive RTU 3d printed samples

Materials used. Unrefined rapeseed oil (RO) was purchased from a local producer, "Iecavnieks" (Latvia), and used as is. N-Hexane, boron trifluoride diethyletherate (BF3•OEt2), NaHCO3, acrylic acid, 1-ethyl-3-methylimidazolium acetate (EmimAc), 2-Hydroxyethyl Methacrylate (HPMA) were supplied by Sigma Aldrich. Photoinitiator (PI) ethyl (2,4,6-trimethylbenzoyl)phenylphosphinate was purchased from FluoroChem. Single-walled carbon nanotubes (SWCNT) were purchased from Tubal (Average diameter 2 nm, length > 5 μm) and used as received.

Acrylated Rapeseed oil synthesis. RO was mixed with acrylic acid in a ratio of 1 to 1 (w/w), and afterwards a syringe was used to add BF3•OEt2 to the original mixture in a 1 to 20 (w/v) ratio, followed by stirring at 80 °C for 5 h. The chilled mixture was washed with n-hexane and a saturated $NaHCO_3$ solution. The water layer was separated, and the remaining hexane was

removed via rotary. The resulting product, acrylated rapeseed oil (ARO), was yellow and transparent.

3D printing resin preparation. ARO and HPMA were first magnetically mixed for 15 min in a ratio of 7 to 3 (w/w) and formed the basis of a bio-based resin. Simultaneously, the desired amount of SWCNTs was added to a fixed amount of IL (1 to 20 ratio (w/w) to bio-based resin). Next, the desired amount of SWCNT was added to the ARO/HPMA mixture and ultrasonicated for 15 min. As the last step, PI was added in a ratio of 3 to 100 (w/w) to the bio-based resin. Finally, the resulting resin was homogenized with a high-shear mixer (Silverson L5M-A, 5000 RPM) for another 20 min. No solvents were used for resin preparation.

3D printing process. 3D printing of electrically conductive samples was performed on an Elegoo Mars 2 PRO (M2P) resin digital light processing (DLP) printer. The printing time was optimized for every formulation by raising the irradiation time until successful printing was possible; the resulting printing times are shown in Table 1. The layer height was set to a constant 50 µm. Compositions with SWCNT loadings of 0.5 wt% and 1 wt% were printed manually, recoating the vat (using the wiper principle) as their viscosities were too high for self-recoating. After printing, prepared samples were washed in isopropanol and post-cured for 10 min using an Original Prusa Curing and Washing Machine (CW1, PRUSA research, Czech Republic).

3.3.2 Bio-based composites with carbon nanotubes and iron oxide nanoparticles

All the materials used in this work are available commercially. Polybutylene suc-cinate (PBS) FZ71PM, injection-moulding grade pellets, were purchased from PTT MCC Biochem Co. Ltd., (Bangkok, Thailand). PBS is a semi-crystalline thermoplastic polyester with a density of 1.26 g/cm^3, MFI 22 g/10 min (190°C, 2.16 kg); it is entirely biodegradable and partially bio-based (50—85%, DIN certification 8C084). Multiwall carbon nanotubes (MWCNT) NC7000™ (density 1.85 g/cm^3, l/d 158) were purchased from Nanocyl SA, (Sambreville, Belgium). Iron (II,III) oxide nanoparticles (Fe_3O_4) (density 5.1 g/cm3, aver-age particle size 100 nm) were purchased from US Research Nanomaterials, Inc., (Hou-ston, TX, USA). Surfactant Ester 80DA (density 1.102 g/cm3) is a water- and sol-vent-soluble synthetic aliphatic ester purchased from ADDAPT Chemicals BV, (Hel-mond, The Netherlands). Chloroform (CAS No.: 67-66-3) (≥99%) was purchased from Merck KGaA, (Darmstadt,

Germany). PBS pellets were dried in a vacuum oven (J.P. Se-lecta, Barcelona, Spain) before use, according to the manufacturer's recommendation (70 °C, 24 h). Nanoparticles were used as received without any further purification and stored in sealed packaging.

The nanocomposites were prepared via a solvent casting process. PBS pellets were dissolved in 150 ml of chloroform (concentration 12.5 g/100 ml). At the same time, nanofillers and the surfactant were dispersed in 100 ml of chloroform and then mixed for 45 min using an ultrasonic sonotrode Hielscher UIS250V (Hielscher Ultrasonics GmbH, Teltov, Germany) and magnetic stirring. The prepared solution and dispersion were combined and homogenised using magnetic stirring for 2 h at 62 °C. The resulting solution (about 150 ml) was cast in a Petri dish in a fume hood and left to evaporate overnight. Any leftover solvent was removed by vacuum drying (24 h at 70 °C). Composite films for testing were prepared using compression moulding (135 °C, 5 min) (Carver Inc.,Wabash, IN, USA), followed by rapid cooling between steel plates to room temperature (22 °C).

3.3.4 Epoxy resin composites

EPIKOTE™ Resin 828 was used as composite matrix. EPIKOTE Resin 828 is a medium viscosity liquid epoxy resin produced from bisphenol A resin and epichlorhydrin. It contains no diluent. EPIKOTE 828 provides good pigment wetting and good resistance to filler settling and a high level of mechanical and chemical resistance properties in cured state. Several series of composite samples, using Epikote 828, a curing agent called A1 (i.e., a modified TEPA) and 0.25, 0.5, 1, 1.5 and 2 wt. % of various carbon fillers were fabricated as follows. The resin was degassed under vacuum (1–3 mbar) for 12-14 h, then was put into an oven at 65°C. In the meantime, the carbon filler was dispersed in propanol, and the suspension was submitted to an ultrasonic bath for 1.5 h. afterwards, the alcoholic suspension of carbon was mixed with the resin. The obtained mixture was placed inside an oven at 130–150°C for evaporating the alcohol. The curing agent A1 was added to the mixture of resin and filler through slow manual mixing for about 7 min. The blend was then poured into moulds of dimensions 1 cm 1 cm 7 cm, and left as such for 20 h for the curing process at room temperature, and finally for 4 h in an oven at 80°C. When the process was completed, the samples were removed from the moulds.

The following carbon particles were used as fillers in epoxy resin:

artificial graphites flakes, kindly supplied by Timcal G+T (Switzerland) under the name TIMREX® KS, were also used: fine graphite (FAC), having mean flake diameters between 15 and 44 µm. Commercially available ENSACO conductive carbon blacks were kindly supplied by Timcal Ltd. (Bodio, Switzerland). Carbon Black of Low surface area - CBL (ENSACO 250 G: BET surface area = 65 m^2/g; oil absorption = 190 mL/100g) was used. Commercially available SWCNT (http://www.nanotubeseu.com/nano/products/s4402/main.html) were used for epoxy resin composites preparation.

4 Result and discussion

4.1 Epoxy resin composites

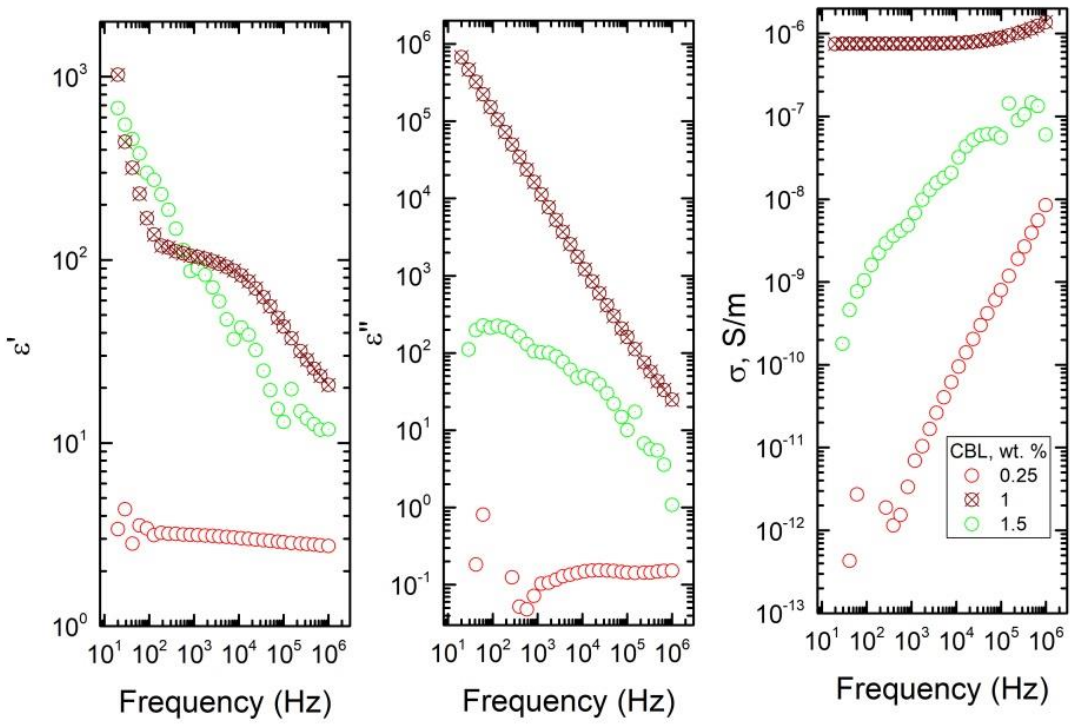

Figure. 4 Dielectric permittivity real part (ε'), imaginary part (ε'') and electrical conductivity σ dependence from frequency for epoxy resin composites with CBL (carbon black) inclusions at different concentrations.

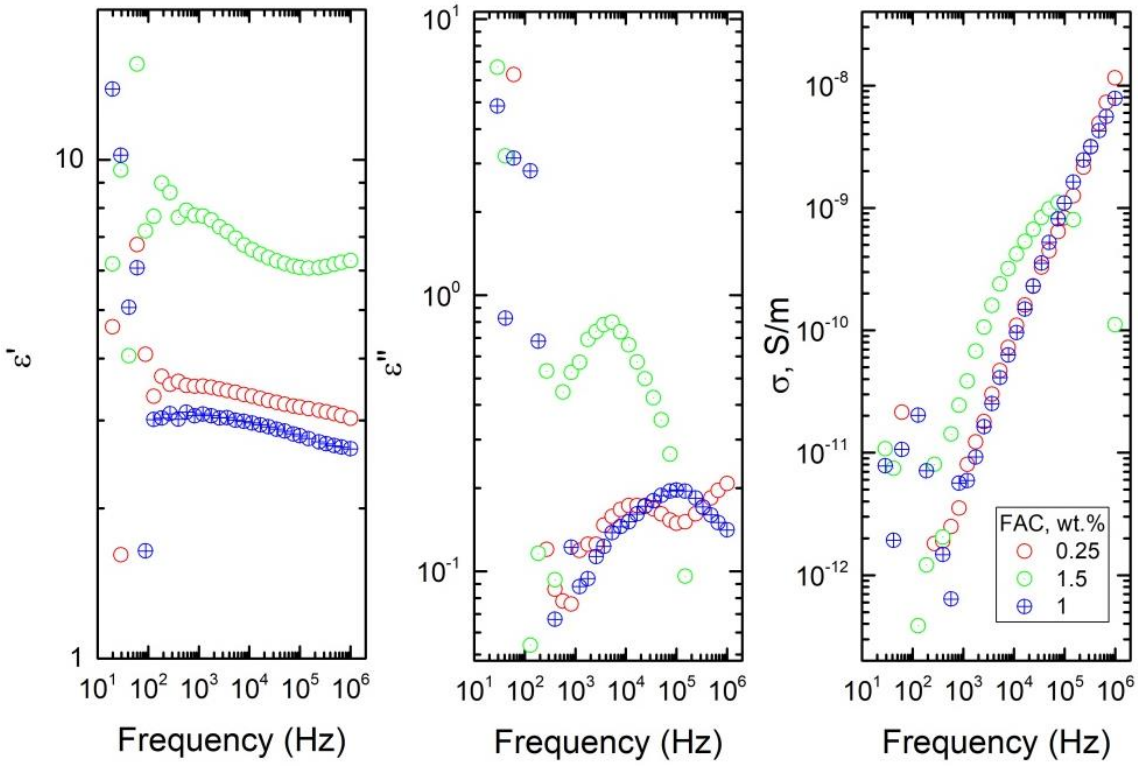

Figure. 5 Dielectric permittivity real part (ε') and imaginary part (ε'') dependence from frequency for epoxy resin composites with FAC (fine activated carbon) inclusions.

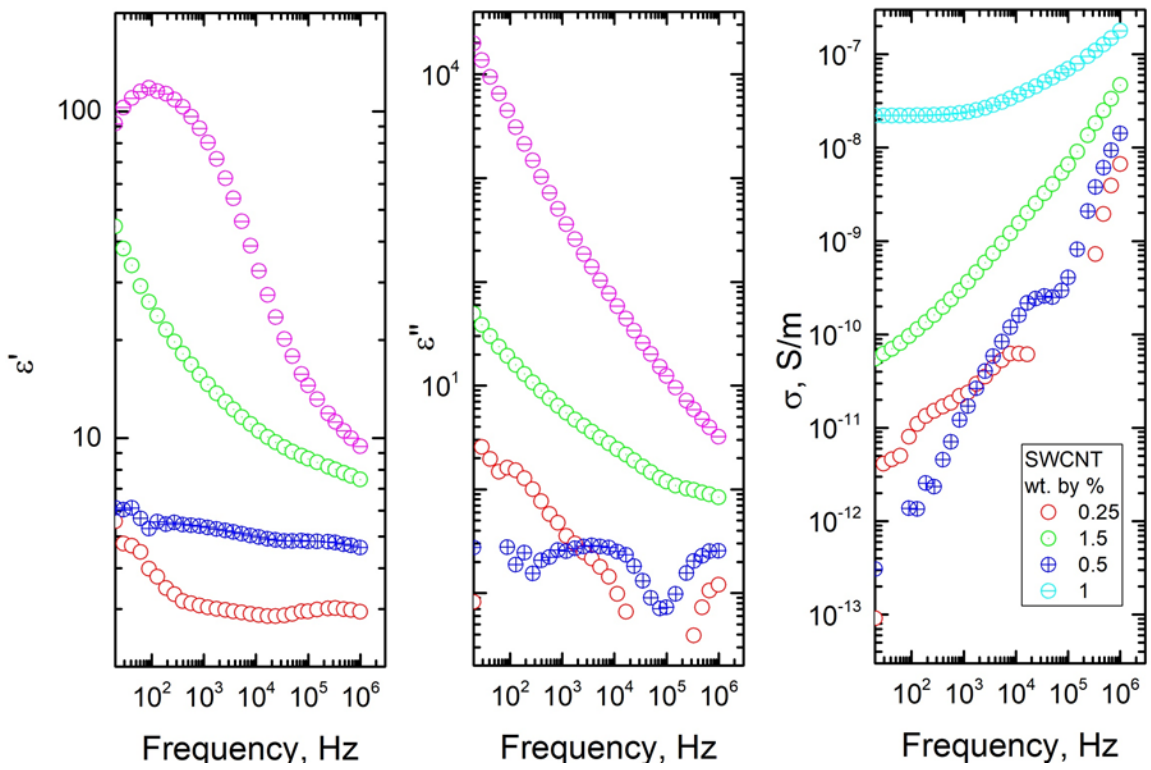

Figure. 6 Dielectric permittivity real part (ε') and imaginary part (ε'') dependence from frequency for epoxy resin composites with single wall carbon nanotubes.

Frequency dependence of complex dielectric permittivity an electrical conductivity for epoxy resin composites with CBL, FAC and SWCNT inclusions are presented in Figs.5-7. It can be concluded that dielectric/electric properties of epoxy resin composites with FAC inclusions are low enough and similar to pure epoxy resin properties (dielectric permittivity are lower than 10, while dielectric losses are lower than 1). The similar behavior is observed for composites with CBL and SWCNT inclusions with concentrations lower than 1 wt. %. Therefore can be concluded that the percolation threshold in composites with CBL and SWCNT inclusions is close to 1 wt %.

4.2 Low frequency dielectric properties of bio-based composites

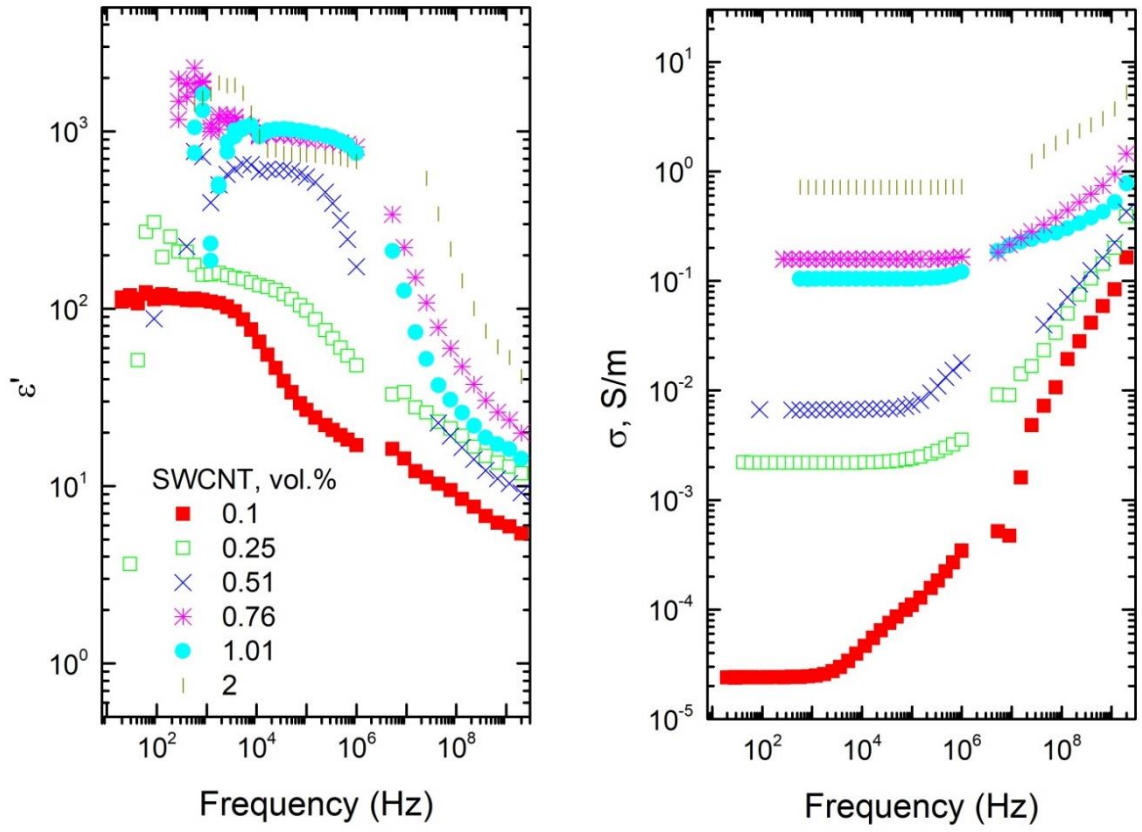

Figure. 7 Frequency dependences of the dielectric permittivity and the electrical conductivity for bio-based composites with SWCNT in 20 Hz – 3 GHz frequency range.

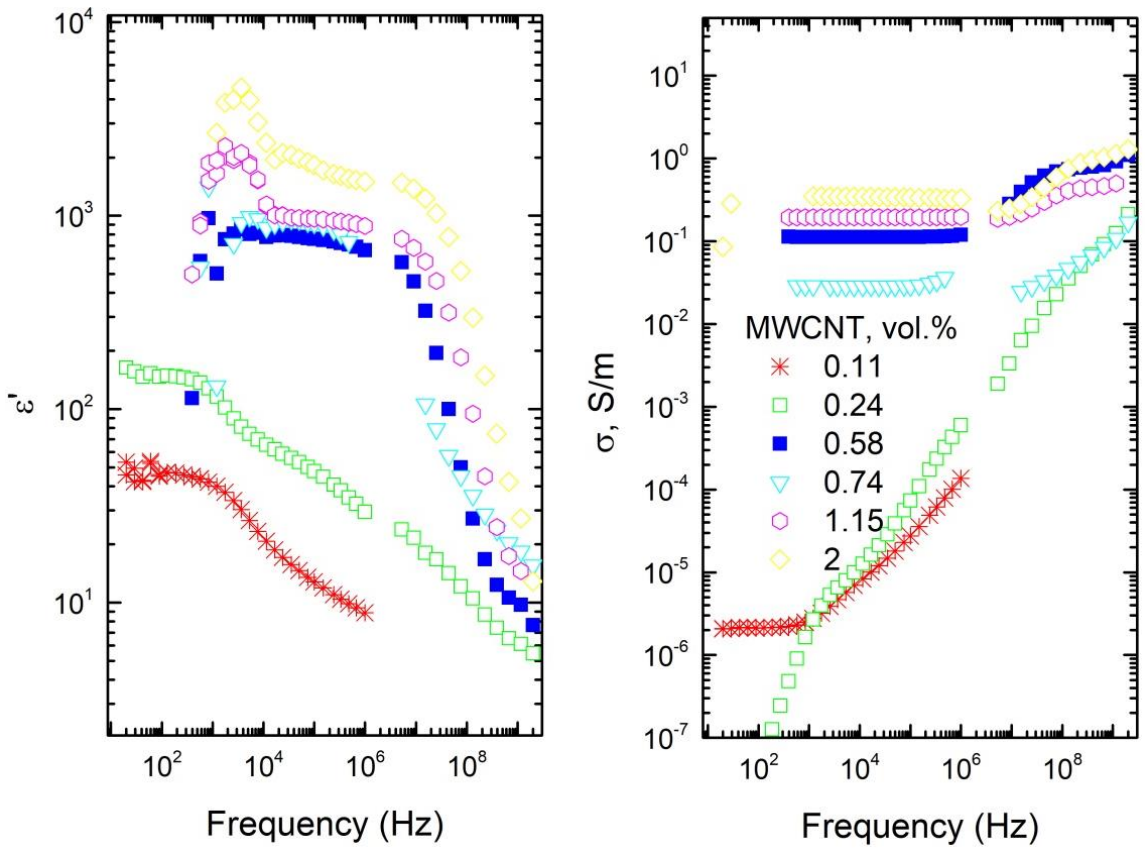

Figure. 8 Frequency dependences of the dielectric permittivity and the electrical conductivity for composites with MWCNT in 20 Hz – 3 GHz frequency range.

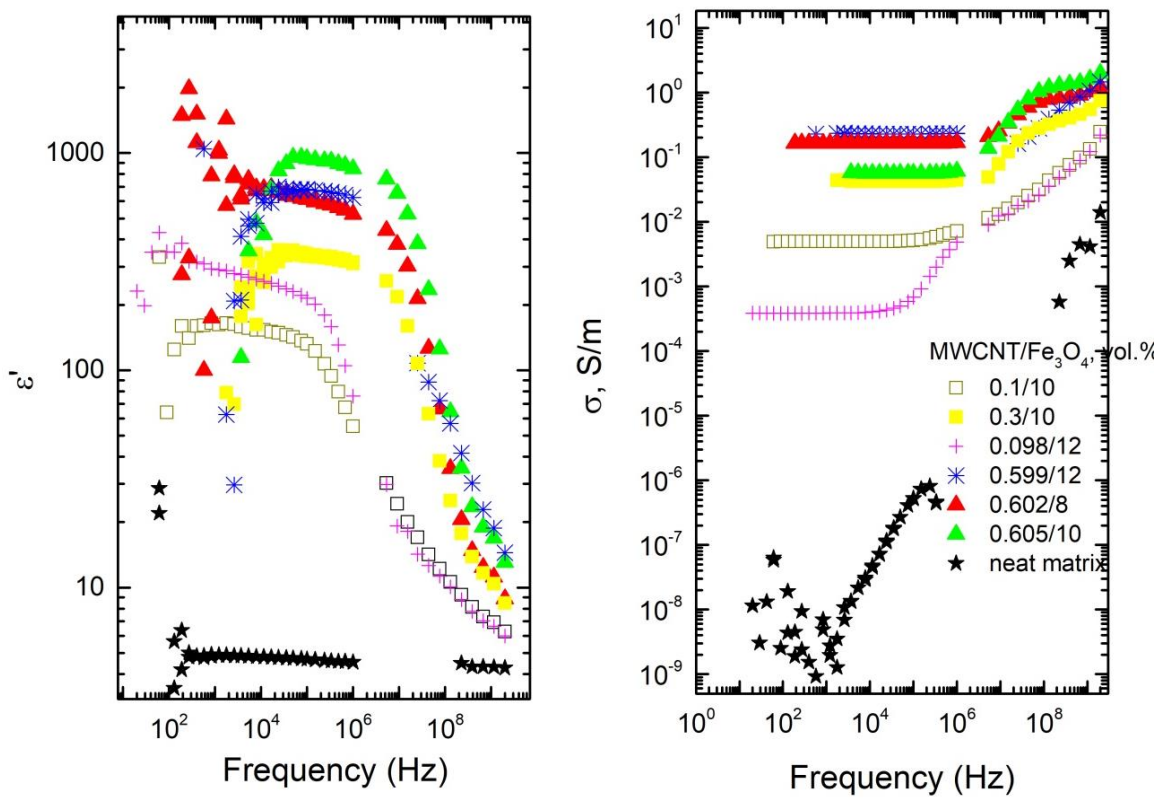

Figure. 9 Frequency dependences of the dielectric permittivity and the electrical conductivity for composites with MWCNT/Fe3O4 in 20 Hz – 3 GHz frequency range.

Frequency dependences of the dielectric permittivity and the electrical conductivity in frequency range 20 Hz – 3 GHz are presented in Fig.7-9. Electrical conductivity spectra have the plateau (frequency independent part) for composites with SWCNT for concentrations not less as 0.1 vol.%, for composites with MWCNT for concentrations not less as 0.11 vol.% and for hybrid composites for all investigated concentrations. Therefore, it possible to conclude that the percolation threshold in the system with SWCNT or MWCNT is close to 0.1 vol.%.

4.3 Microwave dielectric properties of bio-based composites

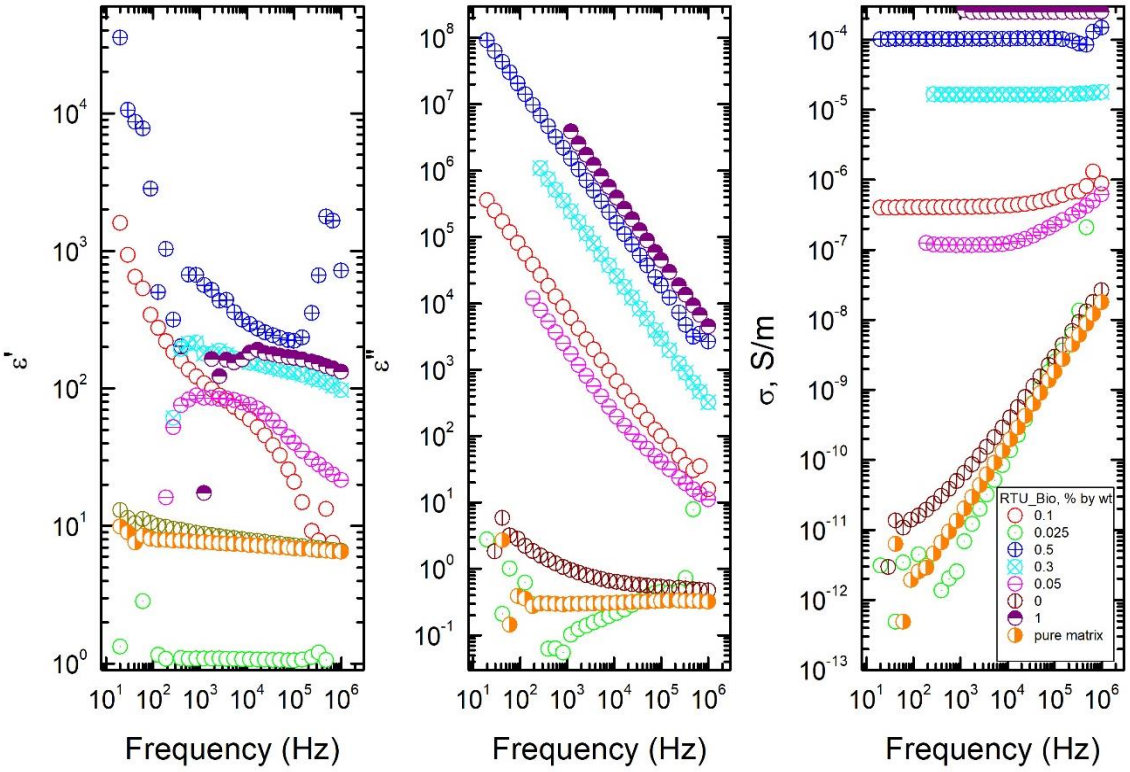

Figure. 10 Dielectric permittivity real part (ε') and imaginary part (ε'') dependence from frequency for bio-based composites.

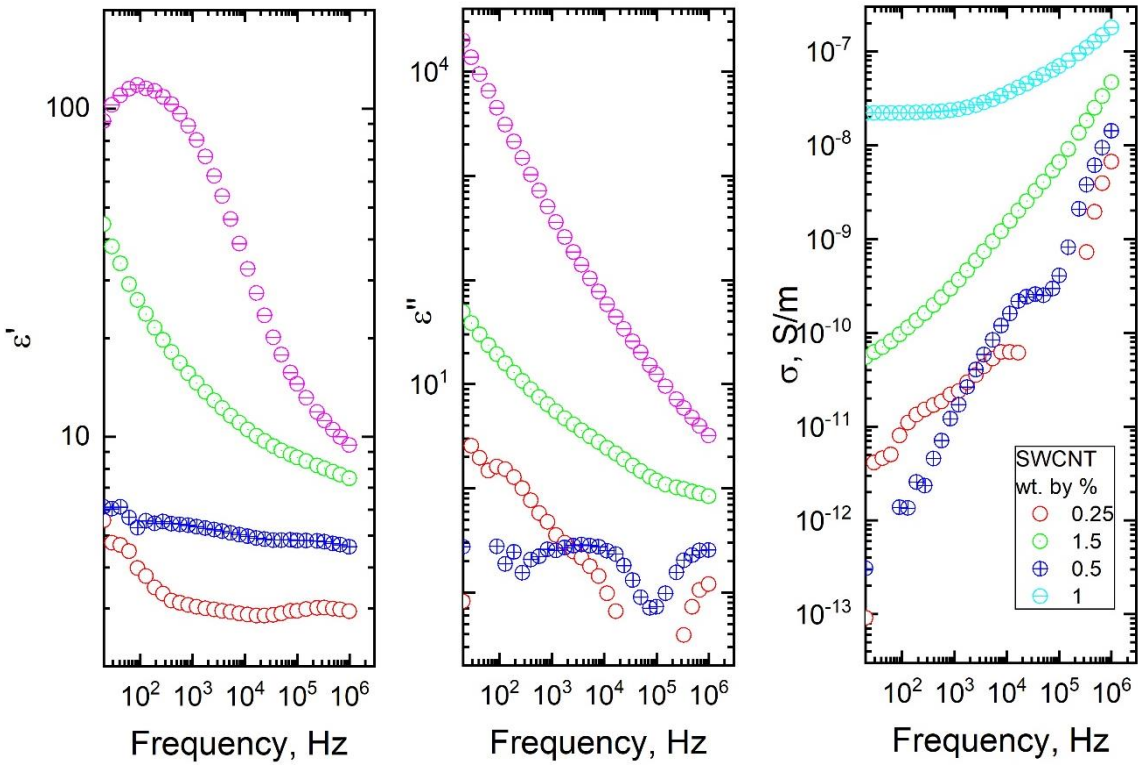

Figure. 11 Dielectric permittivity real part (ε') and imaginary part (ε'') dependence from frequency for samples bio-based composites with SWCNT.

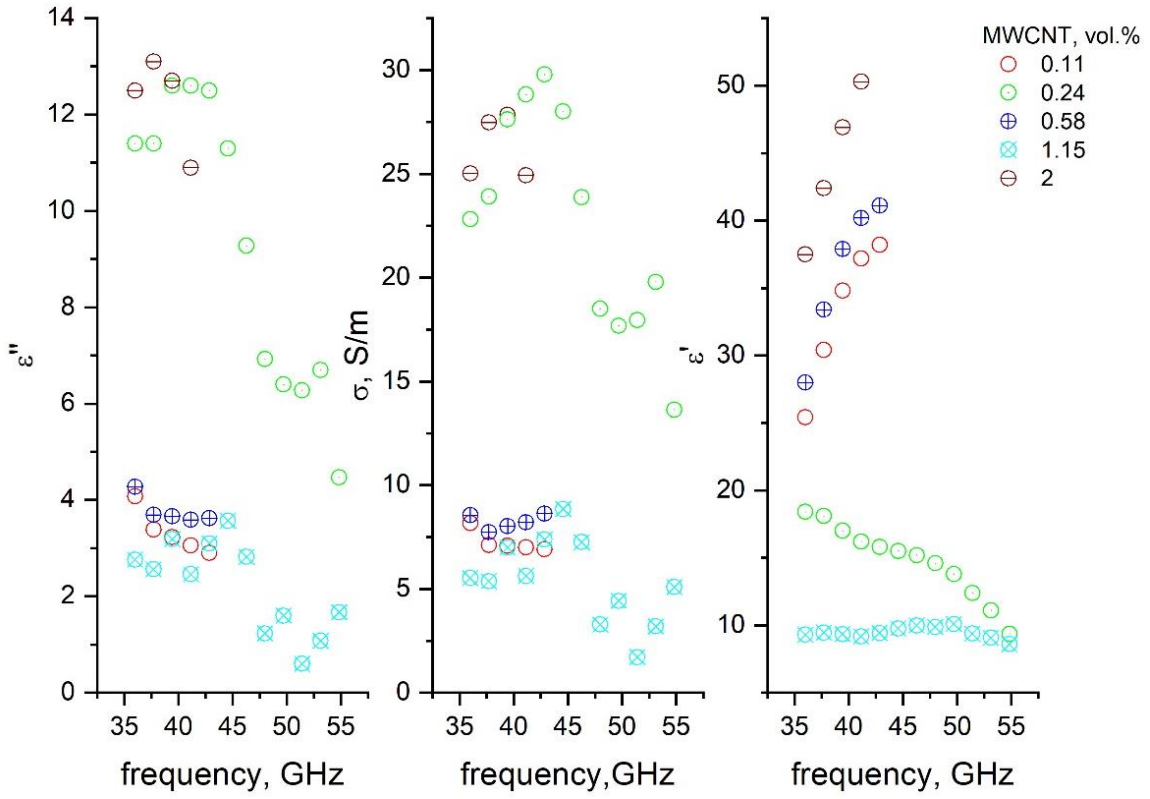

Figure.12 Dielectric permittivity real part (ε') and imaginary part (ε'') dependence from frequency for biobased composites with MWCNT.

Microwave dielectric properties of biobased composites with various inclusions are presented in Figs. 10-12. It can be concluded that microwave dielectric properties of biobased composites with various inclusions are quite good and these composites can be used for various microwave applications. Even at low concentrations, multiwalled carbon nanotubes (MWCNTs) can form interconnected networks within composites and exhibit excellent electrical properties. As a result, incredibly electrically conductive composites can be produced. MWCNTs can create a three-dimensional network of methods within a non-conductive matrix material due to their high aspect ratio and conductivity. An huge improvement in electrical conductivity is achieved by this network's efficient transmission of electrons. MWCNT composites are highly desirable for purposes requiring high electrical conductivity at low filler loadings because they have a lower percolation threshold than other conductive fillers. Electronics, coatings, shielding, interconnects, sensors, and energy storage devices are among the few of the industries where these composites are utilized.

4.4 Reflectivity, transmission and absorption microwave properties of bio-based composites

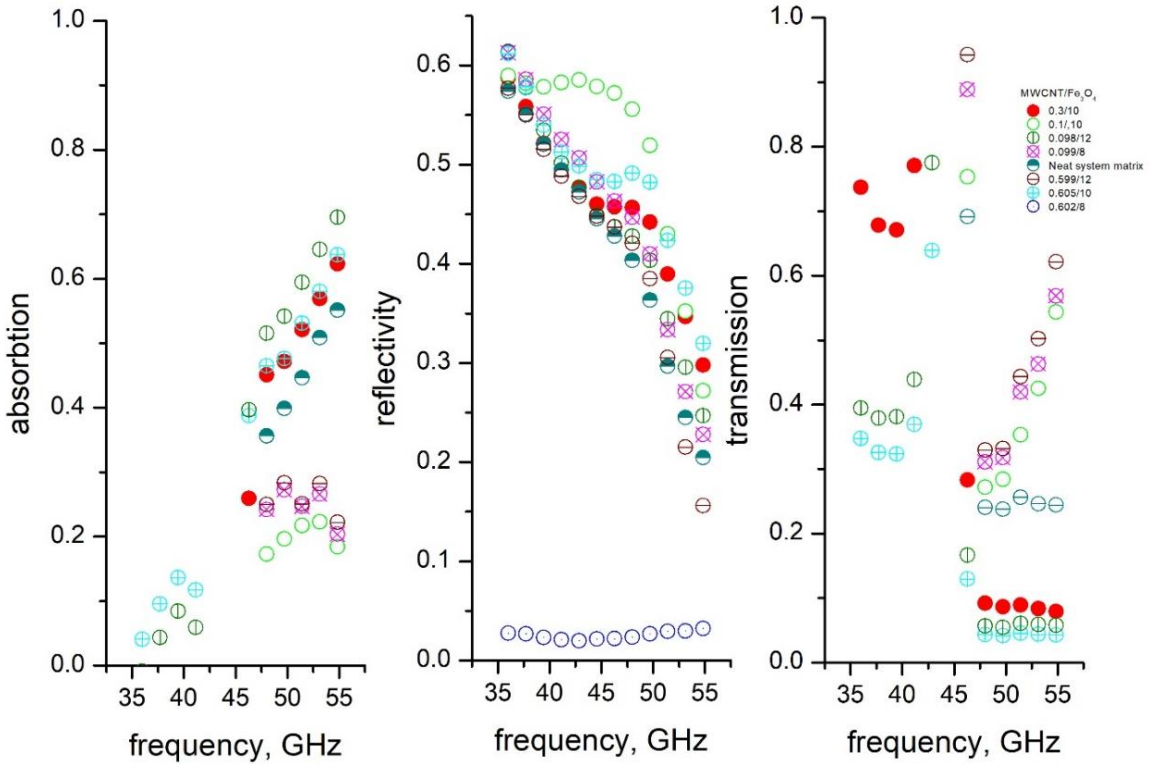

Figure. 13 Reflection, transmission and absorption dependence from frequency for hybrid bio-based composites with Fe_3O_4/MWCNT inclusions.

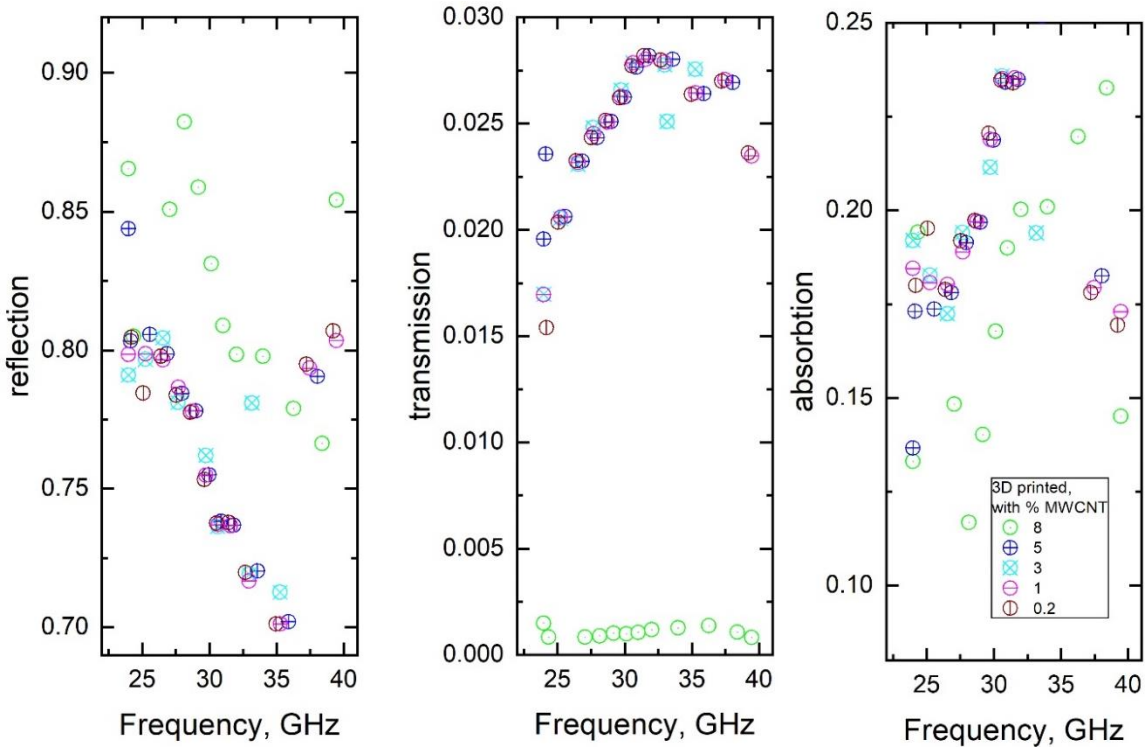

Figure. 14 Reflection, transmission and absorption dependence from frequency for MWCNT biobased composites.

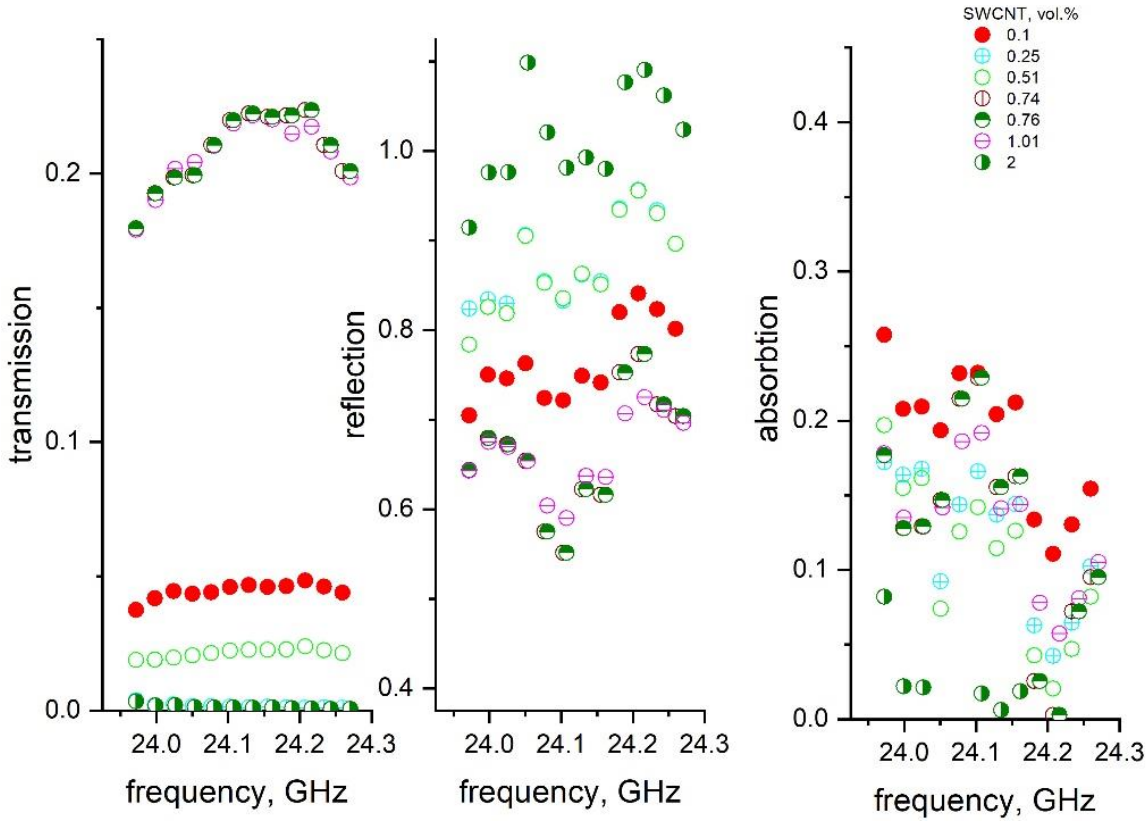

Figure. 15 Reflection, transmission and absorption dependence from frequency for SWCNT bio-based composites.

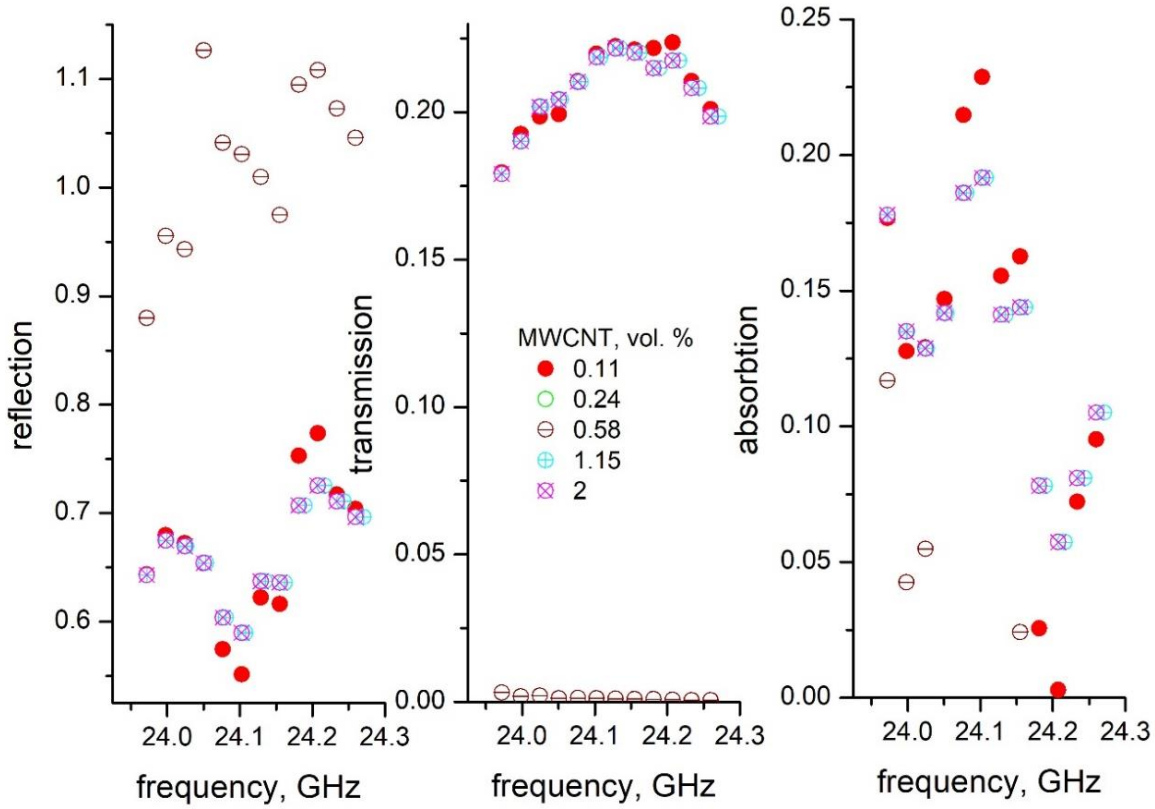

Figure. 16 Reflection, transmission and absorption dependence from low frequency for MWCNT biobased composites.

Figures 13–16 show the frequency dependencies of transmission, reflectivity, and absorption of composites containing Iron-Oxide (size 20 and 100 nm), SWCNT, and MWCNT inclusions as a function of frequency (frequency range 24-35 GHz Ka band) and (35–55, part of V band). For measurements, plate-like samples covering the entire waveguide cross-section and having a thickness of about 0.5 mm were used. For electromagnetic shielding applications, composites with biodegradable matrix and filler concentrations greater than the percolation threshold are suitable. For various electromagnetic applications, hybrid MWCNT/Fe_3O_4 composites (Fig. 13) with absorption values greater than 0.5 demonstrate the most interesting absorption characteristics.

Hybrid MWCNT/Fe_3O_4 composites exhibit significant microwave absorption in the range of 35-53 GHz (significantly larger than 0.5), making them suitable for electromagnetic shielding applications. Additionally, for hybrid MWCNT/Fe_3O_4 composites, the complex dielectric permittivity at uniform MWCNT concentration is highest in the frequency range 26-40 GHz.

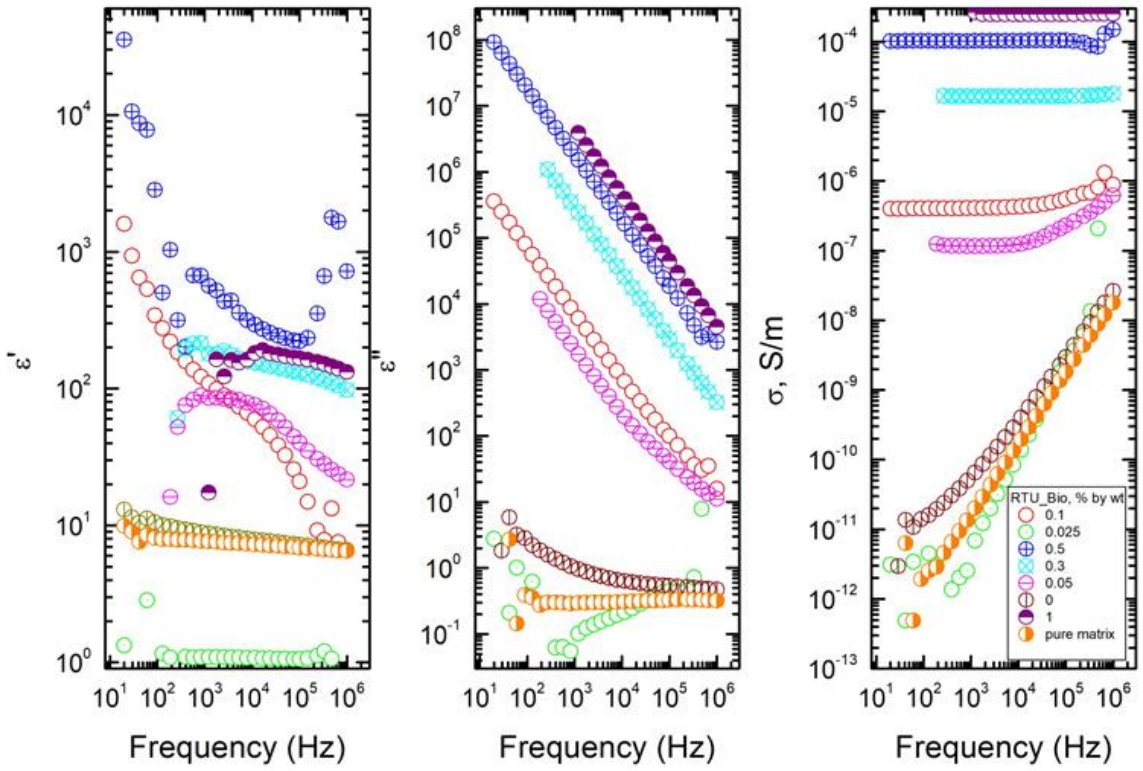

Figure. 17 Dielectric permittivity real part (ε') and imaginary part (ε'') dependence from frequency of RTU 3D printed composites.

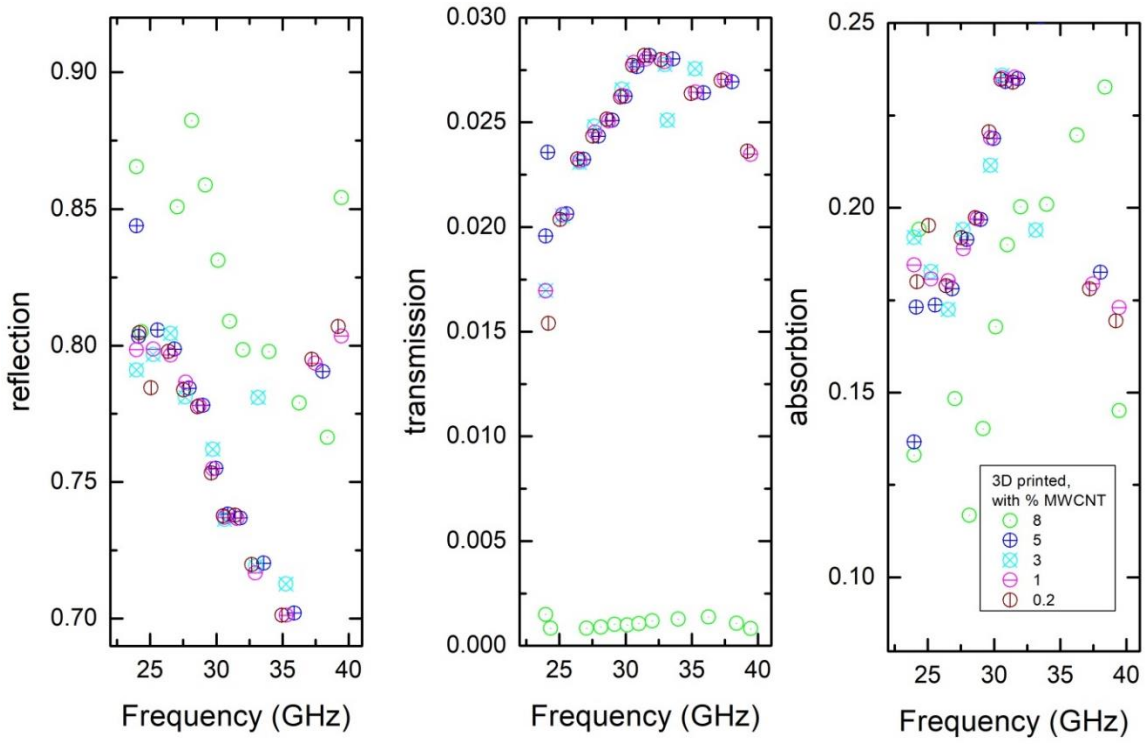

Figure. 18 Reflection, transmission and absorption of RTU 3d printed composites.

Dielectric properties of RTU 3d printed composites are presented in Fig. 17. It can be concluded that the percolation threshold in the system is close to 0.1 vol.%. Reflection, transmission and absorption of RTU 3d printed composites are presented in Fig. 18. Reflection values of these structures are quite high (about 0.7-0.8), while transmission values are quite low (lower as 0.03), at the same time absorption values are about 0.2-0.25. Therefore these structures are suitable for electromagnetic shielding applications.

4.5 Terahertz spectra of bio-based composites

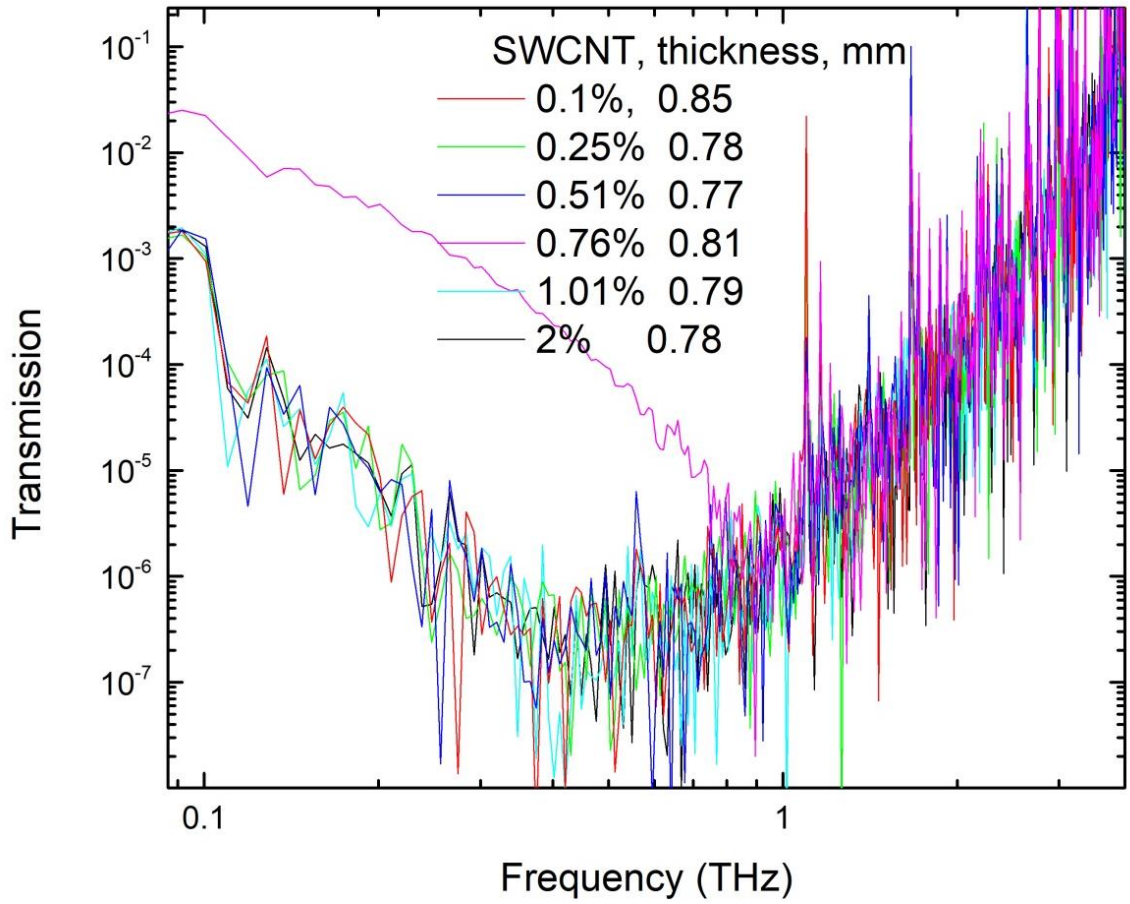

Figure. 19 Time domain spectroscopy transmittance spectra for SWCNT biobased composites.

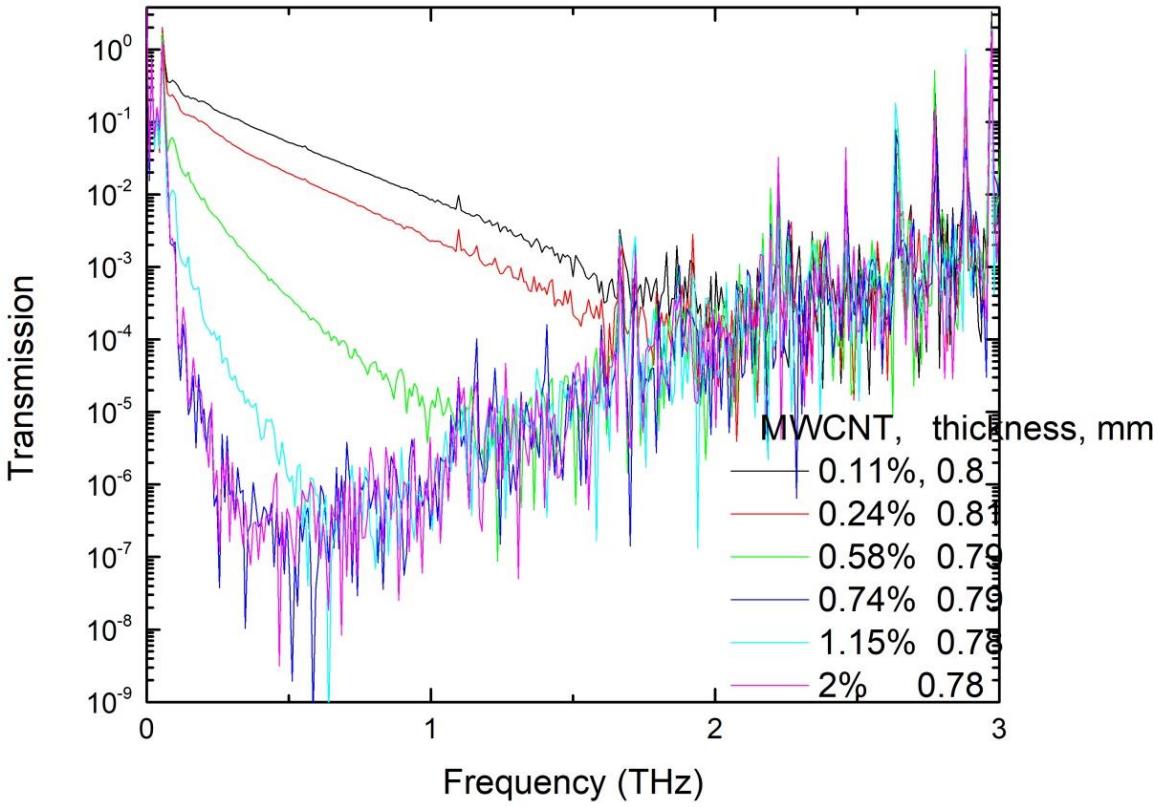

Figure. 20 Time domain spectroscopy transmittance spectra for MWCNT bio-based composites.

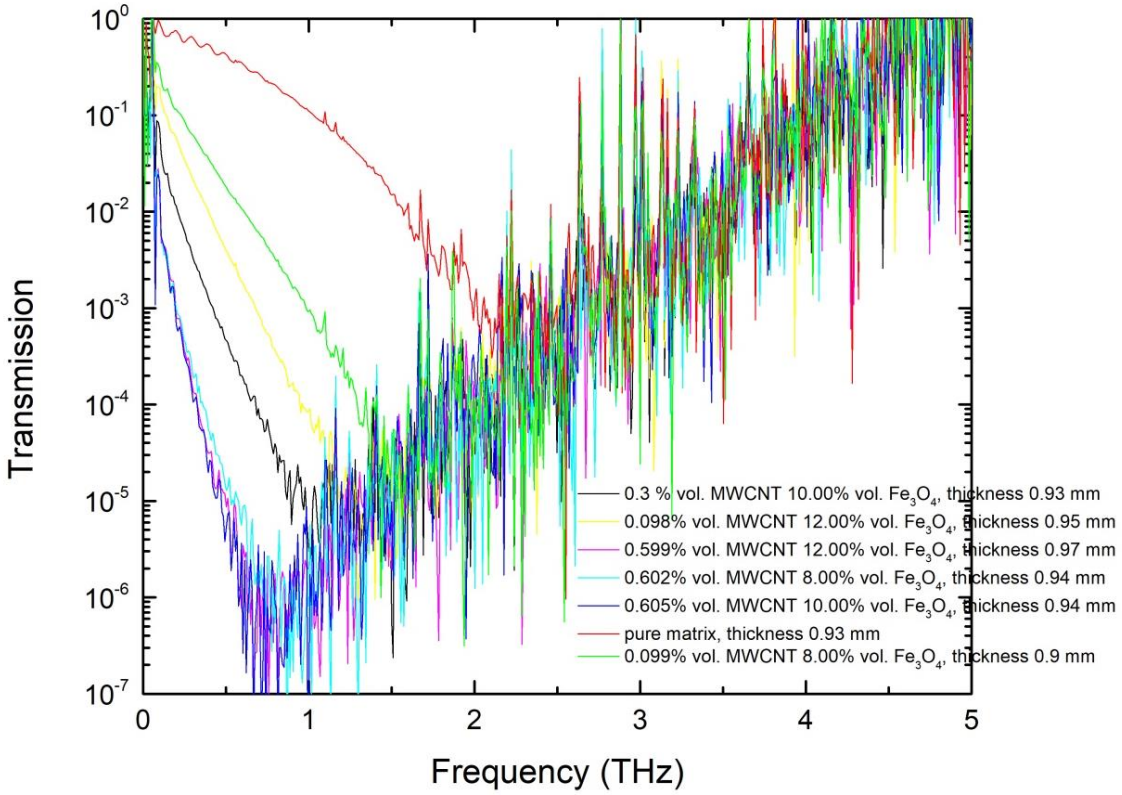

Figure. 21 Time domain spectroscopy transmittance spectra for hybrid MWCNT/ Fe_3O_4 bio-based composites.

Figures 19-21 show the transmission spectra of bio-based composites filled with MWCNT, SWCNT, and hybrid MWCNT/Fe_3O_4 in the terahertz frequency range (100 GHz–3 THz). All composites' transmission firmly decreases with frequency and attains a minimum at some critical frequency. As there is no transmitted signal at higher frequencies, the increase in transmission above the critical frequency is more of a myth. In actuality, single composites with MWCNT concentrations of 0.74 and 2% vol. and hybrid composites with 0.6% vol. MWCNT and numerous Fe_3O_4 nanoparticle concentrations are invisible in the entire terahertz frequency range. With an increase in the concentration of different fillers (MWCNT, SWCNT, or Fe_3O_4), the transmission also reduces. Due to powerful effects between various nanoparticles, hybrid MWCNT/Fe_3O_4 composites with a fixed MWCNT concentration retain terahertz radiation more than composites with MWCNT alone (Fig. 20).

5. Conclusions

1) The electrical percolation of biobased composites with carbon nanotubes inclusions can be quite low (about 0.1 vol.%), similarly or even better than for epoxy composites with carbon nanotubes inclusions.

2) Hybrid MWCNT/Fe_3O_4 composites demonstrate the big microwave absorption in frequency range 35-53 GHz (bigger as 0.5), therefore these materials can be used for electromagnetic shielding applications. Moreover, in frequency range 26-40 GHz the complex dielectric permittivity at fixed MWCNT concentration is biggest for hybrid MWCNT/Fe_3O_4 composites.

3) At fixed MWCNT concentration the absorption of terahertz radiation is bigger in hybrid MWCNT/Fe_3O_4 composites than in composites with MWCNT only, due to strong synergy effects between different nanoparticles.

6. References

1. Kim, G. M., Nam, I. W., Yang, B., Yoon, H. N., Lee, H. K., & Park, S. (2019). Carbon nanotube (CNT) incorporated cementitious composites for functional construction materials: The state of the art. *Composite Structures*, *227*, 111244.
2. Huang, X., Qi, X., Boey, F., & Zhang, H. (2012). Graphene-based composites. *Chemical Society Reviews*, *41*(2), 666-686.
3. Mourdikoudis, S., Kostopoulou, A., & LaGrow, A. P. (2021). Magnetic nanoparticle composites: synergistic effects and applications. *Advanced Science*, *8*(12), 2004951.
4. Tao, H., Amsden, J. J., Strikwerda, A. C., Fan, K., Kaplan, D. L., Zhang, X., ... & Omenetto, F. G. (2010). Metamaterial silk composites at terahertz frequencies. *Advanced materials*, *22*(32), 3527-3531.
5. Bansal, N. P., & Lamon, J. (2014). *Ceramic matrix composites: materials, modeling and technology*. John Wiley & Sons.
6. https://en.wikipedia.org/wiki/Allotropes_of_carbon
7. https://en.wikipedia.org/wiki/Fullerene
8. Bauhofer, W., & Kovacs, J. Z. (2009). A review and analysis of electrical percolation in carbon nanotube polymer composites. *Composites science and technology*, *69*(10), 1486-1498.
9. Feng, C., & Jiang, L. (2013). Micromechanics modeling of the electrical conductivity of carbon nanotube (CNT)–polymer nanocomposites. *Composites Part A: Applied Science and Manufacturing*, *47*, 143-149.
10. Psarras, G. C. (2018). Fundamentals of dielectric theories. In *Dielectric Polymer Materials for High-Density Energy Storage* (pp. 11-57). William Andrew Publishing.
11. Morsalin, S., & Phung, B. T. (2019). Modeling of dielectric dissipation factor measurement for XLPE cable based on Davidson-Cole model. *IEEE Transactions on Dielectrics and Electrical Insulation*, *26*(3), 1018-1026.
12. Batra, S., Unsal, E., & Cakmak, M. (2014). Directed Electric Field Z-Alignment Kinetics of Anisotropic Nanoparticles for Enhanced Ionic Conductivity. *Advanced Functional Materials*, *24*(48), 7698-7708
13. Meisak, D. (2021). *Hybrid multifunctional composites with nanoinclusions and structures for electromagnetic applications* (Doctoral dissertation, Vilniaus universitetas).
14. Kong, L., Yin, X., Xu, H., Yuan, X., Wang, T., Xu, Z., ... & Fan, H. (2019). Powerful absorbing and lightweight electromagnetic shielding CNTs/RGO composite. *Carbon*, *145*, 61-66.
15. Ren, F., Yu, H., Wang, L., Saleem, M., Tian, Z., & Ren, P. (2014). Current progress on the modification of carbon nanotubes and their application in electromagnetic wave absorption. *RSC Advances*, *4*(28), 14419-14431
16. Thomassin, J. M., Jerome, C., Pardoen, T., Bailly, C., Huynen, I., & Detrembleur, C. (2013). Polymer/carbon based composites as electromagnetic interference (EMI) shielding materials. *Materials Science and Engineering: R: Reports*, *74*(7), 211-232.
17. Danlée, Y., Bailly, C., & Huynen, I. (2014). Thin and flexible multilayer polymer composite structures for effective control of microwave electromagnetic absorption. *Composites science and technology*, *100*, 182-188.
18. Welp, U., Kadowaki, K., & Kleiner, R. (2013). Superconducting emitters of THz radiation. *Nature Photonics*, *7*(9), 702-710.
19. Meisak, D. (2021). *Hybrid multifunctional composites with nanoinclusions and structures for electromagnetic applications* (Doctoral dissertation, Vilniaus universitetas).

20. Kerker, M. (2016). *The scattering of light and other electromagnetic radiation*. Elsevier.
21. Dianah, A. R. S. N., Hazmin, S. N., Umar, R., Jaafar, H., Kamarudin, M. K. A., Dagang, A. N., & Syafiqah, H. N. (2018). Spatial model of public non-ionizing radiation exposure on selected base station around Kuala Nerus. *Journal of Fundamental and Applied Sciences*, *10*(1S), 523-540
22. Violante-Carvalho, N., Arruda, W. Z., Carvalho, L. M., Rogers, W. E., & Passaro, M. (2021). Diffraction of irregular ocean waves measured by altimeter in the lee of islands. *Remote Sensing of Environment*, *265*, 112653
23. El-Hajjar, M., & Hanzo, L. (2013). A survey of digital television broadcast transmission techniques. *IEEE Communications surveys & tutorials*, *15*(4), 1924-1949.
24. Violette, N. (2013). *Electromagnetic compatibility handbook*. Springer
25. Urbancokova, H., Kovar, S., Halaska, O., Valouch, J., & Pospisilik, M. (2018). Conditions for testing effects of radiofrequency electromagnetic fields on electronic device. *WSEAS Transactions on Environment and Development*, *14*, 145-152.

Resume

This work is devoted for comparison of electrical properties of epoxy resin and biobased composites with various carbon nanoinclusions. It was demonstrated that percolation threshold values are similar in both systems. In the work were also investigated electromagnetic properties of biobased composites with various carbon and iron oxide nanoinclusions. It was demonstrated that these composites are suitable for electromagnetic shielding applications in microwave and THz frequency ranges. Moreover in the hybrid biobased composites with carbon and iron oxide nanoparticles strong synergy effects were observed. They are related with strong electromagnetic shielding performance enhancement due to the addition of iron oxide nanoparticles.

Santrauka

Šis darbas yra skirtas palyginimui elektrinių savybių epoksidinės dervos ir biopolimerų kompozitų su įvairiais anglies nanodariniais. Yra parodyta, kad perkoliacijos slenkstis abejuose sistemuose yra palyginamas. Taip pat buvo ištirtos biopolimerų kompozitų su įvairiais anglies ir geležies oksido nanodariniais elektromagnetinės savybės mikrobangų ir teraherciniame dažnių diapazone. Nustatyta, kad esant pakankamai anglies nanodarinių koncentracijai kompozitai yra tinkami elektromagnetinių bangų slopinimui plačiame mikrobangų ir teraherciniame dažnių diapazone. Hibridiniems kompozitams su anglies ir geležies oksido nanodariniais pastebėtas sinergijos efektas mikrobangų ir teraherciniame dažnių diapazone. Šis efektas pasireiškia stipresnė elektromagnetinių bangų absorbcija hibridiniuse kompozituose negu kompozituose vien tik su anglies nanodariniais, esant tai pačiai anglies nanodarinių koncentracijai.